

# We are IntechOpen, the world's leading publisher of Open Access books Built by scientists, for scientists

6,000

Open access books available

148,000

International authors and editors

185M

Downloads

Our authors are among the

154

Countries delivered to

TOP 1%

most cited scientists

12.2%

Contributors from top 500 universities



WEB OF SCIENCE™

Selection of our books indexed in the Book Citation Index  
in Web of Science™ Core Collection (BKCI)

Interested in publishing with us?  
Contact [book.department@intechopen.com](mailto:book.department@intechopen.com)

Numbers displayed above are based on latest data collected.  
For more information visit [www.intechopen.com](http://www.intechopen.com)



# Gas Slippage in Tight Formations

*Sherif Fakher and Abdelaziz Khlaifat*

## Abstract

In order to address the gas slippage for flow through tight formation, with a very low porosity (less than 10%) and permeability in micro-Darcy range, a series of single-phase gas flow experiments were conducted. Two different gases ( $N_2$  and He) were used to carry out many single-phase experiments at different overburden and pressure drops and were compared with carbon dioxide ( $CO_2$ ) flow types. The pore size distribution measurements showed the existence of a wide range of pore size distribution. Also, the single-phase gas flow experiments through the core plug, mostly at low pressure, showed Knudsen diffusion type, which is an indication of gas molecules' slippage at the wall of the pores.

**Keywords:** tight formation, slip effect, Knudsen diffusion, non-Darcy flow, pore size distribution

## 1. Introduction

Due to its high compressibility, gas flow behavior can vary greatly as the porous media size varies. Understanding this behavior and the type of flow is vital for the oil and gas industry, especially with the increase in production from unconventional reservoirs with extremely low permeability.

The flow behavior in pores can be estimated using many different mathematical models and experiments, the majority of which used the Knudsen number definition [1–3]. Many mathematical models were developed to determine the flow regime in nanopores as a function of adsorption [4, 5], rock permeability [6, 7], and molecular dynamics [8, 9]. All of these models used some form of the Knudsen number definition in their model in order to predict gas flow behavior as a function of different parameters. Many researchers also attempted to model Knudsen diffusion in shale gas reservoirs to determine the recovery potential when the dominant flow regime was Knudsen diffusion [10–13].

One of the main experimental methods to determine gas flow in nanopores relies on understanding the formation properties of the unconventional reservoir. Research has shown that unconventional tight sand gas reservoirs have three distinct features. These include relatively large pores with mineral deposition in the pores that resulted in a reduction in the overall pore diameter, narrow and flat pores that were generated due to alteration of the primary porosity of the rock, and grains supported by ultra-fine micro-matrix particles, usually clays [14–16]. All three of these have a common feature, which is an extremely small average pore diameter, reaching nanoscale in most cases.

This research studies the predominant flow regime that will be observed for gas flow in nanopores of low-permeability unconventional gas reservoirs using tight sandstone cores and three gasses including helium, nitrogen, and carbon dioxide. The research focuses on pores ranging from less than 10 nm in size up to 400 nm. The research relies on experimental analysis of the pores and the definition of the Knudsen number to determine the flow regime for all three gasses.

## 2. Knudsen flow regimes

To determine the flow behavior through pores, one of the most widely used methods is Knudsen number. It can be defined as a ratio between the mean free path and the pore diameter of the porous media through which the fluid is propagating. The mean free path is the distance that the gas molecule travels until it begins colliding with the other gas molecules. It can be defined mathematically as a function of fluid and thermodynamic conditions as shown in Eq. (1) [1–3]:

$$\lambda = \frac{3.2\mu}{p} \sqrt{\frac{PT}{2\pi M}} \quad (1)$$

where  $\lambda$  is the mean free path,  $\mu$  is the viscosity,  $p$  is the pressure,  $T$  is the temperature,  $M$  is the fluid molecular weight, and  $R$  is the universal gas constant.

Knudsen number integrates the mean free path, which includes the fluid and the thermodynamic properties, with the pore size, which is a rock property, to predict the flow behavior of the gas in different pore sizes. Knudsen number is defined mathematically as shown in Eq. (2) [12]:

$$K_n = \frac{\lambda}{2r} \quad (2)$$

where  $K_n$  is the Knudsen number, and  $r$  is the average pore radius or half the pore diameter.

Based on the definition of Knudsen number, there are four possible situations for the gas flow in different pore sizes. These include the following:

- $K_n \geq 10$ : This type of flow is referred to as Knudsen diffusion. This occurs when the mean free path is much larger than the pore diameter. This is the case in small pore sizes, less than 10 nm. Collision between both the gas molecules and the capillary walls is important in this case.
- $10 > K_n \geq 0.1$ : This is known as a transition region. It highlights the beginning of the transition between Knudsen diffusion and normal flow. In this case, the large difference between the mean free path and the pore diameter begins narrowing down. The molecule-wall interactions begin reducing; however, its effect is still significant on the flow.

- $0.1 > K_n \geq 0.01$ : This is known as slip flow. In some cases, this is grouped with the transition flow as one case due to the similarity in behavior. In this case, the mean free path and the pore diameter are comparable with each other. Knudsen number begins decreasing until it is very close to the range of viscous flow, although it has still not reached it. The molecule-molecule and molecule-wall interactions are still both significant in this case.
- $0.01 > K_n$ : This case is referred to as viscous flow. In this case, the mean free path is much smaller than the pore diameter. The molecule-molecule collision becomes predominant, whereas the molecule-wall collision is insignificant. In this case, normal molecular diffusion occurs.

### 3. Experimental description

A description of the material, setup, and procedure followed to conduct all the experiments is explained in this section. All experiments were conducted using the same conditions to be able to accurately compare the results.

#### 3.1 Experimental material

The material used to conduct the experiments include the following:

- *Distilled Water*: Distilled water was used for the displacement of fluids through the accumulator and for some of the saturation experiments.
- *Nitrogen Gas*: Nitrogen gas is provided through high-pressure nitrogen cylinders. The nitrogen was injected and pressurized in the high-pressure vessels for the experiments.
- *Helium Gas*: Helium gas is provided through high-pressure helium cylinders. The helium was injected and pressurized in the high-pressure vessels for the experiments.
- *Sandstone Core Plugs*: Sandstone core plugs from Travis Peak Formation in East Texas collected from a depth of 8700 ft were used to conduct the experiments. The cores were 3.5 inches in length and 1.5 inches in diameter.
- *Stainless Steel Tubing*: The stainless steel tubings were allocated in the setup to create connections between the different high-pressure vessels, the pump, and the core holder.
- *High-Pressure Valves*: High-pressure valves with a pressure limitation of 15,000 psi were used to control the flow of fluids across the setup.
- *Transducers*: High-accuracy transducers that could record pressure, temperature, and flow rate were used in the experiments to log these values for the duration of the experiment.

### 3.2 Experimental setup

The setup used to conduct the gas flow regime through low-permeability porous media is illustrated in **Figure 1**. The setup is composed of a pump used to inject the fluids into four different high-pressure vessels in the core holder. The vessels include water, helium, and nitrogen. The core holder is connected to transducers that measure pressure, temperature, and flow rates. The core holder houses a sandstone core used to mimic the porous media. Valves are allocated across the setup to control the flow direction of different fluids.

## 4. Results

The results for the pore size distribution using both mercury intrusion and gas sorption will be presented. Also, the dominant flow behavior for different pore size ranges will be determined for each of the three gases used in this research.

To determine the flow regime, the Knudsen number definition was used. Since it relies on the mean free path, this was calculated for all three gases. The mean free path for He, N<sub>2</sub>, and CO<sub>2</sub> at ambient conditions is shown in **Table 1**.

### 4.1 Mercury intrusion

Mercury intrusion porosimetry technique involves the measurement of the capillary pressure and volume of mercury that penetrated the sample pores at a specified pressure. Although widely used to determine pore distribution, this method will not detect the pores that are present in necks narrower than the pore itself due to the inability of the mercury to intrude in them.

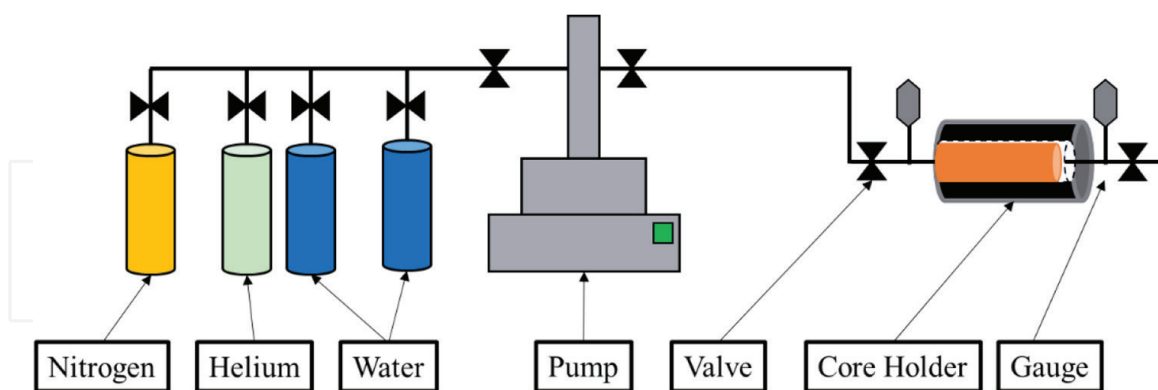


**Figure 1.**  
*Gas flow regime experimental setup.*

Gas type	Mean free path, nm
Nitrogen	67
Helium	195.5
Carbon dioxide	28

**Table 1.**  
*Mean free path for N<sub>2</sub>, He, and CO<sub>2</sub> at ambient conditions.*

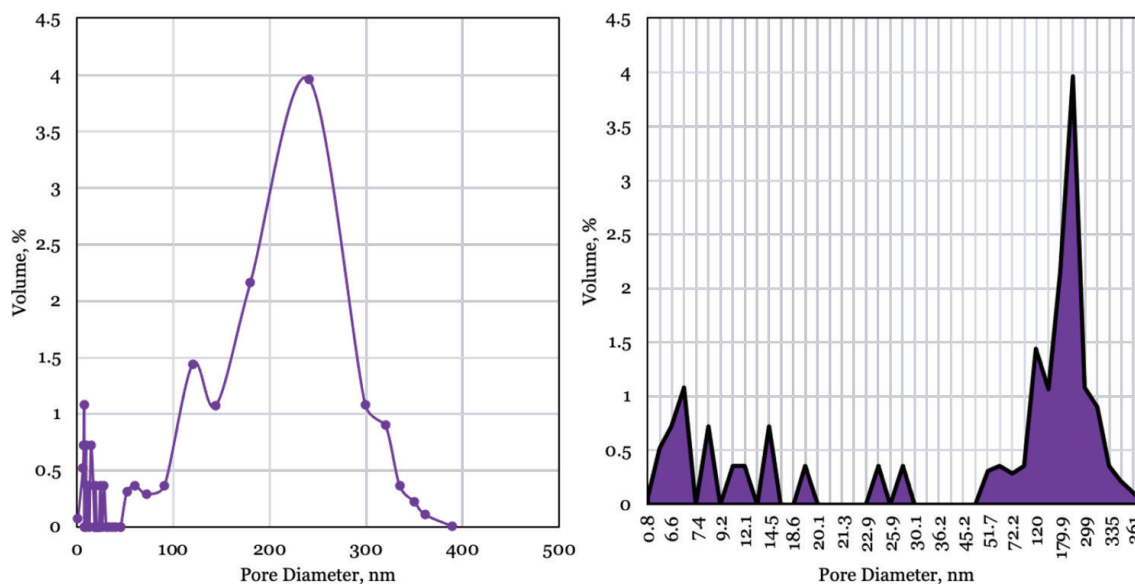


**Figure 2.**  
*Pore size distribution using mercury intrusion.*

#### 4.1.1 Pore size distribution

The pore size distribution using mercury intrusion is presented in **Figure 2**. A wide distribution of pores was available in the core, with the highest volume being for the 180 nm pore size. Based on the available pore sizes and their frequency, the Knudsen number was calculated to determine the predominant flow regime for the helium, nitrogen, and carbon dioxide.

#### 4.1.2 Flow behavior in pores

The flow behavior of all three gasses in the core was evaluated using Knudsen number. Based on the ranges previously discussed, the flow behavior was determined for different pore sizes. The Knudsen number was plotted versus the pore size for three different ranges of pore sizes including up to 10 nm, between 10 and 100 nm, and greater than 100 nm.

The Knudsen number values for the pore size up to 10 nm for all three gasses are shown in **Figure 3**. For all pore sizes, helium exhibits Knudsen diffusion. This is predominantly due to the helium molecular size being small compared with the nitrogen and the carbon dioxide. As for the nitrogen and the carbon dioxide, their flow behavior is very similar, as both exhibit a transition from low Knudsen number to large Knudsen number for the same pore diameter. The main predominant flow behavior for both gasses is transition flow and Knudsen diffusion. This is due to the larger molecular size of both compared with helium.

The Knudsen number values for the pore sizes between 10 and 100 nm for all three gasses are shown in **Figure 4**. It can be observed that the Knudsen number values for all three gasses are decreasing with the increase in pore size. This is due to the increase in the pore diameter relative to the mean free path. For pore sizes greater than 20 nm, Knudsen diffusion disappears entirely for all three gasses. For helium, the flow is dominated by transition flow, whereas for the nitrogen and carbon dioxide, the flow is dominated by transition and slip flow.

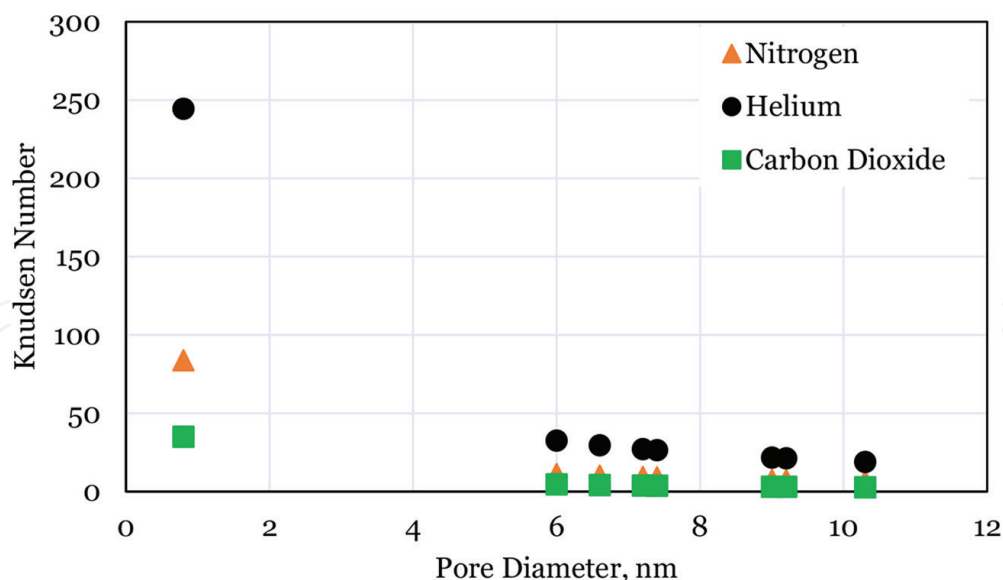


**Figure 3.** Knudsen number for all three gasses for average pore sizes less than 10 nm using mercury intrusion method.

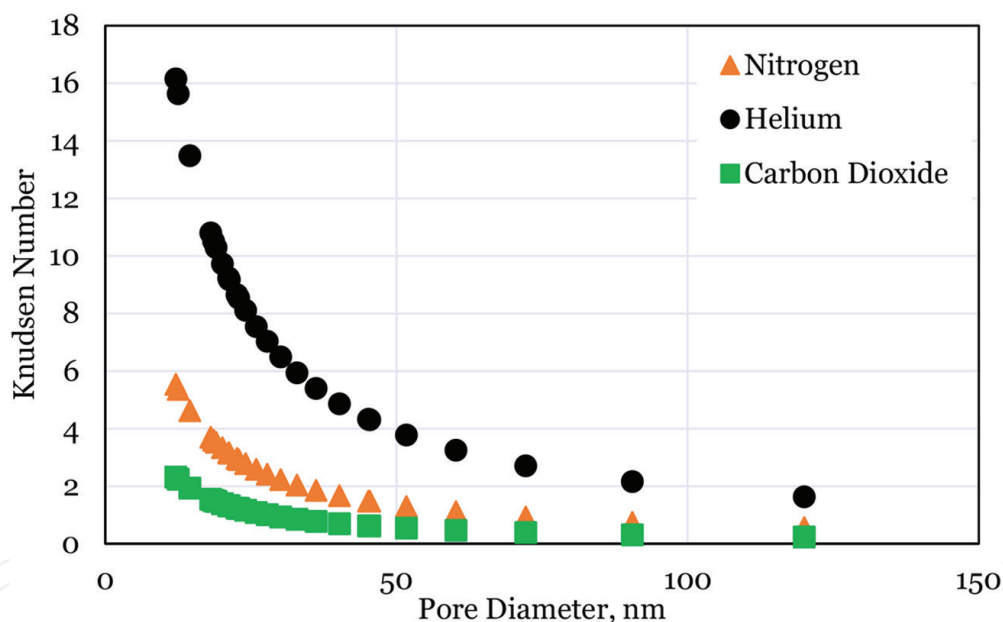


**Figure 4.** Knudsen number for all three gasses for average pore sizes between 10 and 100 nm using mercury intrusion method.

The Knudsen number values for the pore sizes greater than 100 nm for all three gasses are shown in **Figure 5**. For helium, this pore size marks the transition from transition flow to slip flow. As for the nitrogen and carbon dioxide, this pore size range marks the dominance of slip flow and the appearance of molecular diffusion. Since the pore diameter is large compared with the mean free path, the molecule-wall interaction is small compared with the molecule-molecule interaction.

#### 4.2 Gas sorption isotherm

A cylindrical pore model was used to determine the pore size distribution using gas sorption isotherm. This method is accurate for pore sizes ranging between 0.4

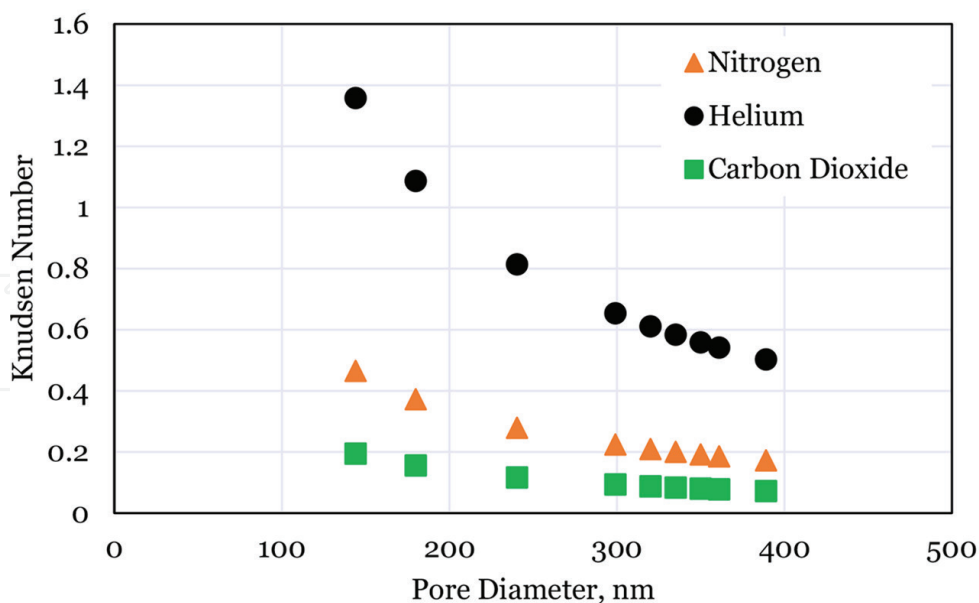


**Figure 5.** Knudsen number for all three gasses for average pore sizes greater than 100 nm using mercury intrusion method.

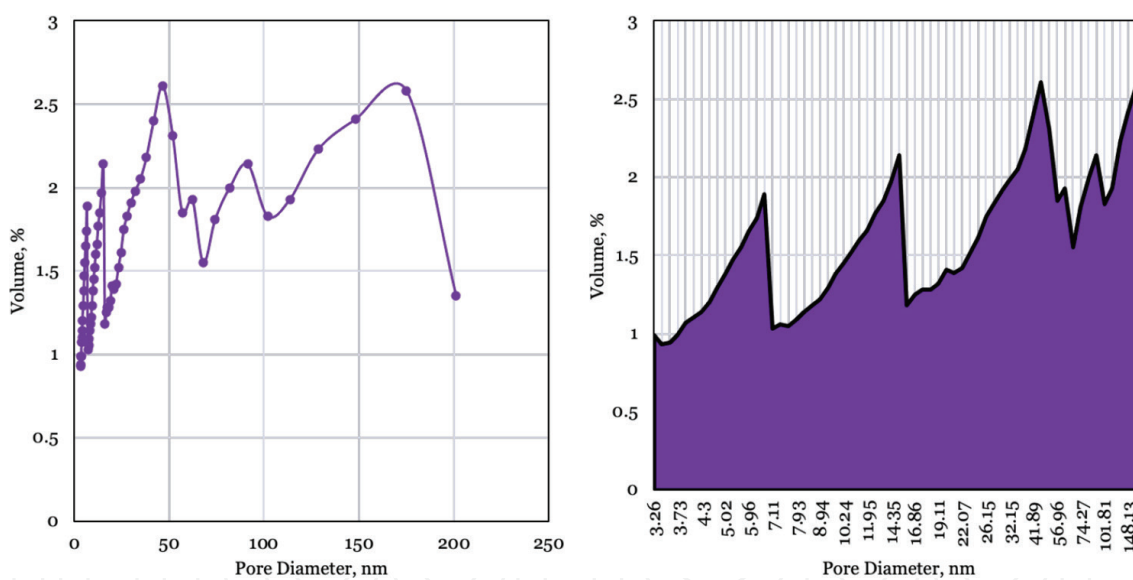


**Figure 6.** Pore size distribution using gas sorption.

and 200 nm. The pore size distribution was determined by analysis of the adsorption isotherm using Kelvin’s equation to correlate the adsorbing gas relative pressure in equilibrium with the porous media.

#### 4.2.1 Pore size distribution

The pore size distribution for the core sample used in this research using gas sorption is shown in **Figure 6**. Compared with the pore size distribution using mercury intrusion, the largest pore size found using the gas sorption method was in the range of 200 nm. The maximum volume of pore sizes was 56 nm.



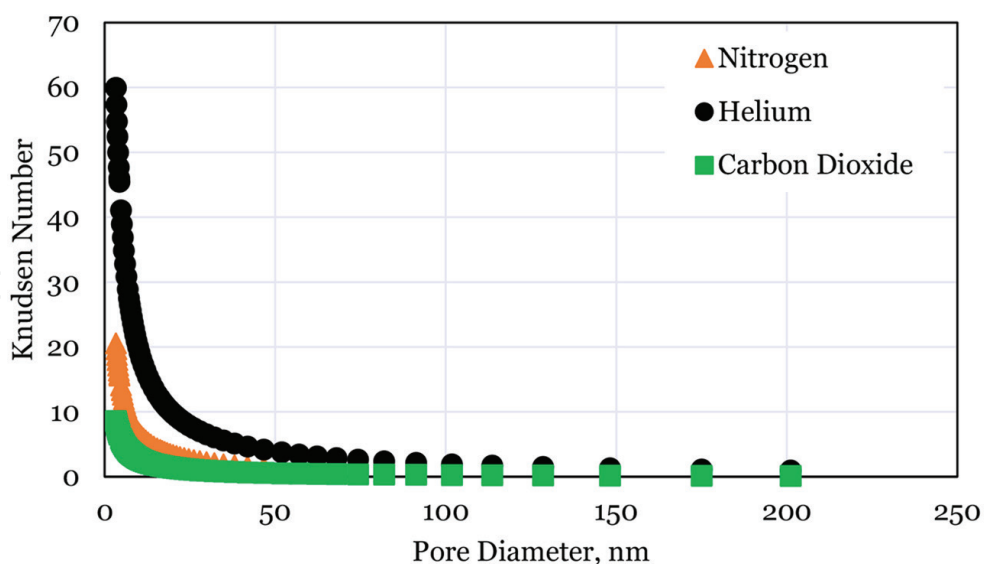


**Figure 7.**  
Knudsen number for all three gasses using gas sorption.

#### 4.2.2 Flow behavior in pores

Similar to the flow behavior analysis using the pore size distribution found via mercury intrusion, the flow regime for all three gases was evaluated using Knudsen number for the pore size distribution obtained using gas sorption. **Figure 7** shows the overall Knudsen number values for all the pore sizes for all three gases. These are then divided into three pore size distributions for clearer analysis. The ranges include pore sizes less than 10 nm, pore sizes between 10 and 100 nm, and pore sizes greater than 100 nm.

The Knudsen number values for all three gasses in pores diameters less than 10 nm are shown in **Figure 8**. For helium, the flow is entirely Knudsen diffusion for diameters

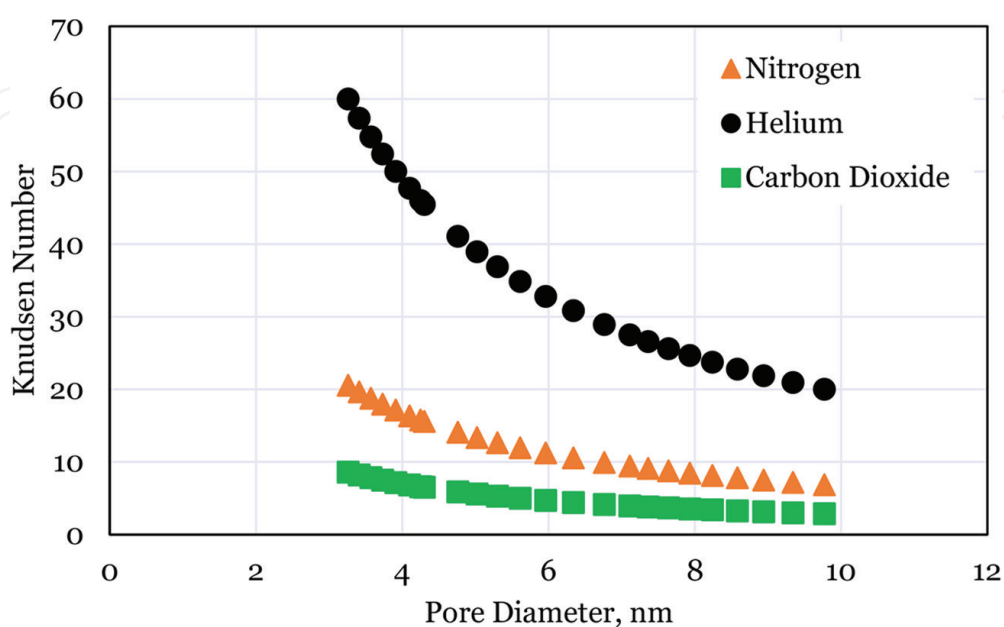


**Figure 8.**  
Knudsen number for all three gasses for average pore sizes less than 10 nm using gas sorption.

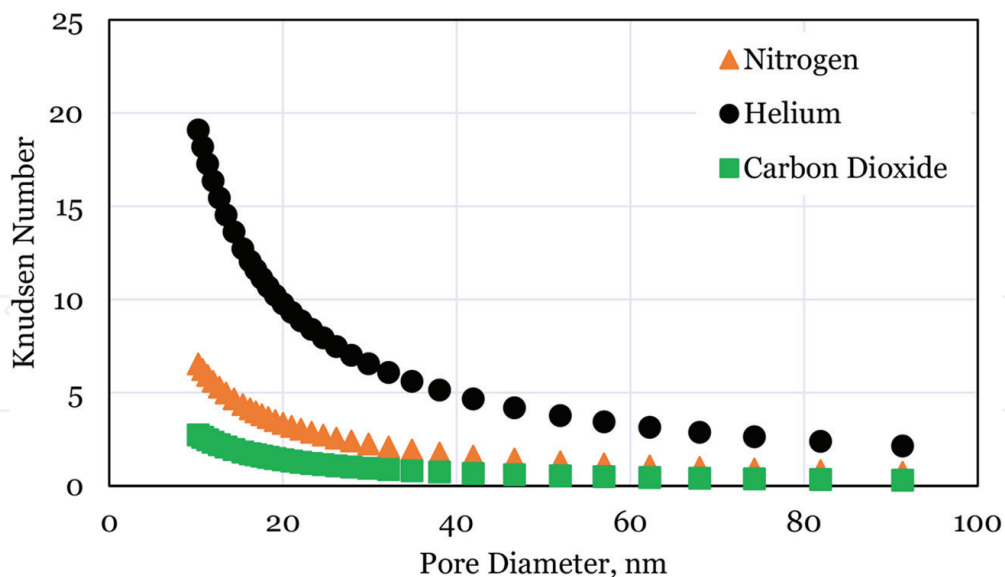


**Figure 9.** Knudsen number for all three gasses for average pore sizes between 10 and 100 nm using gas sorption.

up to 10 nm. Nitrogen exhibits Knudsen diffusion until the pore diameter reaches 6 nm, above which the flow begins to be transition flow. As for the carbon dioxide, the flow begins at transition and does not reach Knudsen diffusion. Since the pore radius is uniform for all three gasses, the main variation that results in the change in the flow regime is the mean free path. The thermodynamic conditions are also the same for all experiments; therefore, the main factor contributing to the variation in the mean free path value is the size of the gas molecule.

The Knudsen number values for all three gasses in pores diameters between 10 and 100 nm are shown in **Figure 9**. The flow behavior for helium begins to shift to transition flow when the pore diameter exceeds 20 nm. For nitrogen and carbon dioxide, the flow behavior is dominated by transition flow. As the pore sizes increase beyond 80 nm, the flow behavior begins approaching slip flow.

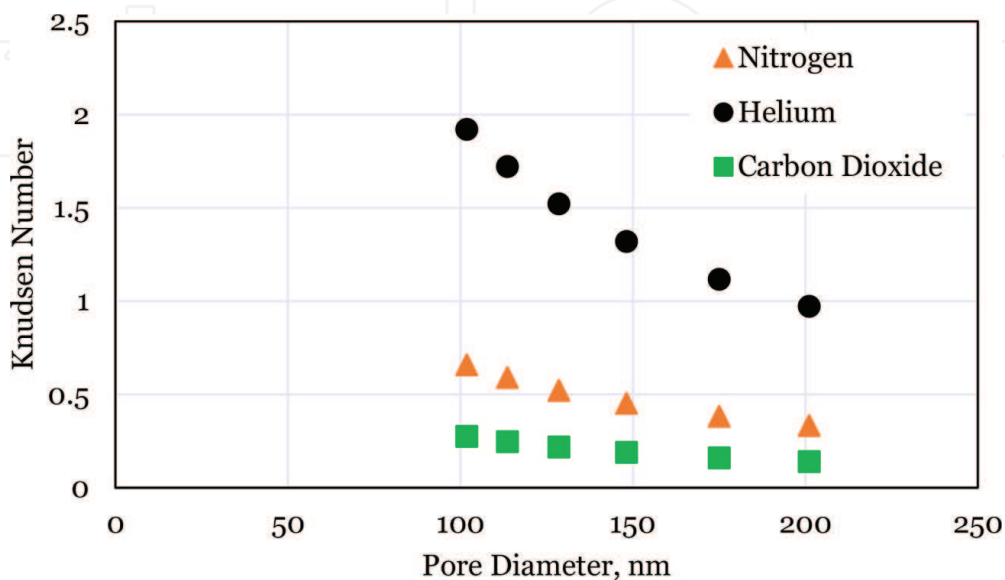


**Figure 10.** Knudsen number for all three gasses for average pore sizes greater than 100 nm using gas sorption.

Measurement method	Average pore size range, nm	Gas type	Dominant flow type
Mercury Intrusion	Less than 10	He	Knudsen diffusion
	10–100		Transition flow
	Greater than 100		Transition flow Slip flow
	Less than 10	N <sub>2</sub>	Knudsen diffusion Transition flow
	10–100		Transition flow Slip flow
	Greater than 100		Slip flow
	Less than 10	CO <sub>2</sub>	Knudsen diffusion Transition flow
	10–100		Transition flow Slip flow
	Greater than 100		Slip flow Molecular diffusion
Gas Sorption	Less than 10	He	Knudsen diffusion
	10–100		Knudsen diffusion Transition flow
	Greater than 100		Transition flow
	Less than 10	N <sub>2</sub>	Knudsen diffusion Transition flow
	10–100		Transition flow
	Greater than 100		Transition flow
	Less than 10	CO <sub>2</sub>	Transition flow
	10–100		Transition flow
	Greater than 100		Transition flow Slip flow

**Table 2.**  
*Knudsen number values for all experiments.*

The Knudsen number values for all three gasses in pores diameters greater than 100 nm are shown in **Figure 10**. For all three gasses, transition flow is the dominant flow behavior in this pore size. The flow regime for carbon dioxide reaches slip flow in the largest pore size observed, whereas, for all other pore sizes, the flow is dominated by transition flow.

#### 4.3 Summary of flow behavior for all three gasses

Based on the analysis of the flow regimes for helium, nitrogen, and carbon dioxide using pore size distribution obtained using mercury intrusion and gas sorption, the predominant flow regime for each gas was determined. In order to determine the change in flow regime with pore size, the pore sizes were analyzed using three different ranges. A summary of the dominant flow regimes for each gas type in different pore sizes is shown in **Table 2**.

## 5. Conclusion

This research investigates the dominant flow regime for three gasses, including helium, nitrogen, and carbon dioxide, in nanopore sizes to determine the most prominent flow behavior present in unconventional gas reservoirs. The research utilizes the Knudsen number definition to determine the flow behavior as a function of the pore diameter size and the mean free path. Based on the results, it was found that in pore sizes less than 10 nm, the dominant flow behavior was Knudsen diffusion, while in pore sizes greater than that, the flow behavior begins to transition from diffusion dominated to viscous-dominated flow, until eventually in the larger pore sizes, the flow is dominated by molecular diffusion.

IntechOpen


### Author details

Sherif Fagher and Abdelaziz Khlaifat\*  
The American University in Cairo, Cairo, Egypt

\*Address all correspondence to: [abdelaziz.khlaifat@aucegypt.edu](mailto:abdelaziz.khlaifat@aucegypt.edu)

### IntechOpen

---

© 2022 The Author(s). Licensee IntechOpen. This chapter is distributed under the terms of the Creative Commons Attribution License (<http://creativecommons.org/licenses/by/3.0>), which permits unrestricted use, distribution, and reproduction in any medium, provided the original work is properly cited. 

## References

- [1] Khlaifat A. Non-Darcy flow in tight gas reservoir of travis peak formation. In: Paper presented at the SPE Middle East Unconventional Gas Conference and Exhibition. Muscat, Oman; 2011
- [2] Khlaifat A, Qutob H, Arastoopour H. Deviation from Darcy's flow in fractured tight gas sand reservoirs. In: Paper presented at the SPE/DGS Saudi Arabia Section Technical Symposium and Exhibition. Al-Khobar, Saudi Arabia; 2011
- [3] Al-Khlaifat A. Two-phase flow through low permeability fractured tight sand porous media (Order No. 9833028). Available from ProQuest Dissertations & Theses Global. (304439510). 1998
- [4] Shabro V et al. Numerical simulation of shale-gas production: From pore-scale modeling of slip-flow, Knudsen diffusion, and langmuir desorption to reservoir modeling of compressible fluid. In: Presented at the SPE North American Unconventional Gas Conference and Exhibition. Woodlands, Texas, USA; 2011
- [5] Shabro V et al. Forecasting gas production in organic shale with the combined numerical simulation of gas diffusion in Kerogen, Langmuir desorption from kerogen surfaces, and advection in nanopores. In: Presented at the 2012 SPE Annual Technical Conference and Exhibition. San Antonio, Texas, USA; 2012
- [6] Gao C et al. The shale-gas permeability measurement considering the rarefaction effect on transport mechanism in the nanopores. In: Presented at the International Petroleum Technology Conference. Beijing, China; 2013
- [7] Niu C et al. Second-order gas-permeability correlation of shale during slip flow. SPE Journal. 2014;**19**:786-792. DOI: 10.2118/168226-PA
- [8] Okamoto N et al. Slip velocity and permeability of gas flow in nanopores for shale gas development. In: Presented at the SPE Asia Pacific Unconventional Resources Conference and Exhibition. Brisbane, Australia; 2015
- [9] Okamoto N et al. Slip velocity of methane flow in nanopores with Kerogen and quartz surfaces. SPE Journal. 2018;**23**: 102-116. DOI: 10.2118/176989-PA
- [10] Wu K et al. A unified model for gas transfer in nanopores of shale-gas reservoirs: Coupling pore diffusion and surface diffusion. SPE Journal. 2016;**21**:1583-1611. DOI: 10.2118/2014-1921039-PA
- [11] Xu J et al. Nanoscale free gas transport in shale rocks: A hard-sphere based model. In: Presented at the SPE Unconventional Resources Conference. Alberta, Canada; 2017
- [12] Fagher S et al. What are the dominant flow regimes during carbon dioxide propagation in shale reservoirs' matrix, natural fractures and hydraulic fractures? In: SPE Western Regional Meeting, Virtual. 2021
- [13] Fagher S et al. Increasing oil recovery from unconventional shale reservoirs using cyclic carbon dioxide injection. In: Paper presented at the SPE Europec, Virtual. 2020
- [14] Sharer JC, O'Shea P. GRI's research program on unconventional natural gas. Chemical Engineering Program. 1986;**82**:19

*Gas Slippage in Tight Formations*  
DOI: <http://dx.doi.org/10.5772/intechopen.106839>

[15] Seoder DJ. Assessing tight gas reservoir quality using petrography and core analysis. In: Proceeding of International Gas Research Conference. 1989

[16] Seoder DJ. Reservoir properties and the pore structure of tight gas sands. AAPG Bulletin. 1984;**64**:4

IntechOpen

IntechOpen